Divalent metal transporter 1 (DMT1) contributes to neurodegeneration in animal models of Parkinson's disease

Julio Salazar[a,b,c], Natalia Mena[c], Stephane Hunot[a,b], Annick Prigent[a,b], Daniel Alvarez-Fischer[a,b], Miguel Arredondo[c], Charles Duyckaerts[a,b], Veronique Sazdovitch[a,b], Lin Zhao[d], Laura M. Garrick[d], Marco T. Nuñez[c], Michael D. Garrick[d], Rita Raisman-Vozari[a,b], and Etienne C. Hirsch[a,b,1]

[a]Institut National de la Santé et de la Recherche Médicale, Neurologie et Thérapeutique Expérimentale, Unité Mixte de Recherche S679, 47 Boulevard de l'Hôpital, 75013 Paris, France; [b]Unité Mixte de Recherche S679, Université Pierre et Marie Curie, Boulevard de l'Hôpital, 75013 Paris, France; [c]Millennium Institute for Cell Dynamics and Biotechnology and Department of Biology, Faculty of Sciences, Universidad de Chile, Las Encinas 3370, Santiago, Chile; and [d]Department of Biochemistry, University at Buffalo, State University of New York, 140 Farber Hall, 3435 Main Street, Buffalo, NY 14214

Dopaminergic cell death in the substantia nigra (SN) is central to Parkinson's disease (PD), but the neurodegenerative mechanisms have not been completely elucidated. Iron accumulation in dopaminergic and glial cells in the SN of PD patients may contribute to the generation of oxidative stress, protein aggregation, and neuronal death. The mechanisms involved in iron accumulation also remain unclear. Here, we describe an increase in the expression of an isoform of the divalent metal transporter 1 (DMT1/Nramp2/Slc11a2) in the SN of PD patients. Using the PD animal model of 1-methyl-4-phenyl-1,2,3,6-tetrahydropyridine (MPTP) intoxication in mice, we showed that DMT1 expression increases in the ventral mesencephalon of intoxicated animals, concomitant with iron accumulation, oxidative stress, and dopaminergic cell loss. In addition, we report that a mutation in DMT1 that impairs iron transport protects rodents against parkinsonism-inducing neurotoxins MPTP and 6-hydroxydopamine. This study supports a critical role for DMT1 in iron-mediated neurodegeneration in PD.

iron | oxidative stress | substantia nigra | MPTP | 6-hydroxydopamine

Parkinson's disease (PD) is the most frequent neurodegenerative movement disorder worldwide. It is characterized by a preferential degeneration of dopaminergic neurons (DNs) in the substantia nigra pars compacta (SNpc) and the presence of proteinaceous cytoplasmic inclusions, called Lewy bodies, in the remaining DNs (1). Apart from rare, inherited forms of the disease, the etiology of PD remains unknown. Nevertheless, it seems clear that aging, mitochondrial dysfunction, inflammation, and oxidative imbalance are among the factors contributing to its pathophysiology.

A rise in iron content localized in glial cells and DNs of the SNpc has been reported in patients with PD (2, 3). This increase of iron is thought to contribute to DN cell death by catalyzing the production of hydroxyl radicals from hydrogen peroxide, a byproduct in dopamine catabolism, and by promoting fibril formation of α-synuclein, the most abundant component of Lewy bodies (4). Neuroprotection achieved by pharmacological or genetic chelation of iron in animal models of PD supports the role of iron in neuronal degeneration in PD (5). Yet, the mechanisms underlying the iron increase have not been elucidated. Transferrin-bound iron (TBI) can be incorporated into cells by an endocytotic process, which is initiated by transferrin receptor 1 (TfR1) ligand binding. Following translocation to early endosomes, iron dissociates from transferrin and is transported to the cytoplasm or directly to the mitochondria. In the brain, iron uptake mediated by TfR participates in iron transport through the blood–brain barrier (6), and the density of TBI-binding sites correlates well with the regional distribution of TfR expression on the luminal surface of endothelial cells. However, TBI-binding sites and TfR expression only loosely correlate with the final steady-state distribution of iron (7). Moreover, TBI-binding sites are decreased in number in the SNpc DNs of PD patients (8).

Non-transferrin-bound iron (NTBI) can be incorporated from the extracellular matrix and/or from the recycling endosomes through the divalent metal transporter 1 (DMT1, Nramp2/Slc11a2), a proton-coupled metal transporter (9). Depending on alternative promoter usage and alternative splicing of 3′ exons, there are 4 DMT1 protein isoforms (10). Two of these contain an iron-responsive element (IRE) in the last exon and 2 do not; the C-terminal DMT1 protein isoforms are thus designated I, or +IRE, and II, or −IRE. A recent study on rat brain reported that the expression of both the +IRE and −IRE DMT1 isoforms is not modulated by iron overload or deficiency and is increased during aging (11), the main risk factor in PD. On the other hand, in vitro studies in multiple cell lines, including monocytes/macrophages (12, 13), bronchial epithelial cells (14), and endothelial cells (15), have shown that the expression of DMT1 is modulated by inflammation, a key phenomenon in the cascade of events leading to neuronal loss in PD (16). Thus, the main aim of this study was to test the hypothesis that changes in DMT1 expression contribute to neurodegeneration in animal models of PD.

We characterized the expression of DMT1 isoforms in substantia nigra (SN) from control and PD patients and the changes in nigral DMT1 expression occurring in mice intoxicated with the mitochondrial complex I inhibitor, 1-methyl-4-phenyl-1,2,3,6-tetrahydropyridine (MPTP), an established model of PD (17). We found that a mutation (G185R) that impairs DMT1 iron transport (18, 19) decreases the susceptibility of microcytic mice (*mk*/*mk*) and Belgrade rats to MPTP-induced and 6-hydroxydopamine (6-OHDA)-induced neurotoxicity, respectively. These observations support the hypothesis that a DMT1-dependent increase in iron plays a role in the death of DNs in PD.

Results

DMT1 Expression in DNs in PD. To evaluate the participation of DMT1 in iron accumulation in the SNpc of PD patients, immunohistochemistry experiments were performed on human

Author contributions: J.S., S.H., L.M.G., M.D.G., and E.C.H. designed research; J.S., N.M., A.P., D.A.-F., M.A., L.Z., and L.M.G. performed research; M.A., C.D., and V.S. contributed new reagents/analytic tools; J.S., S.H., D.A.-F., M.T.N., M.D.G., R.R.-V., and E.C.H. analyzed data; and J.S., L.M.G., M.D.G., and E.C.H. wrote the paper.

[1]To whom correspondence should be addressed. E-mail: etienne.hirsch@upmc.fr.

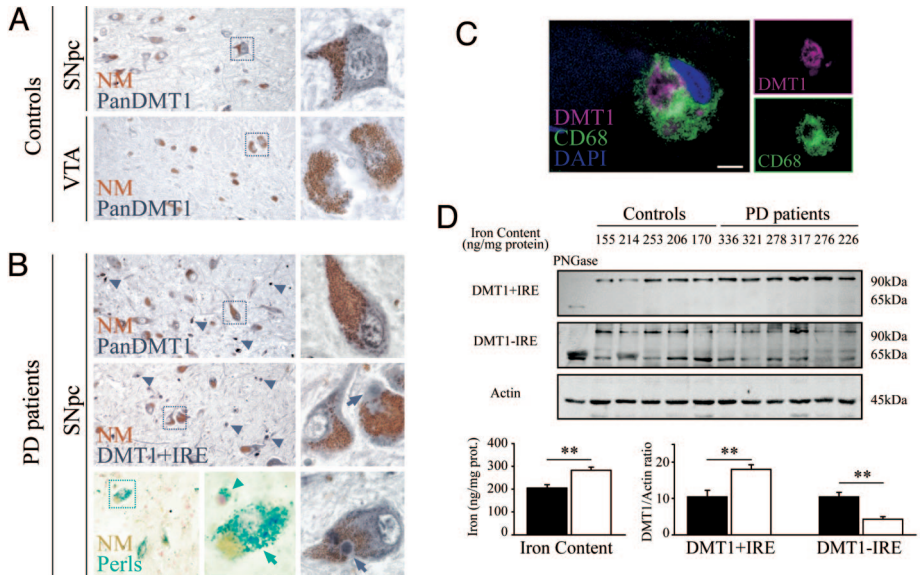

Fig. 1. DMT1 expression in human mesencephalon. (*A*) DMT1 expression in neuromelanin (brown)-containing neurons of control subjects (images representative of 6 subjects studied). Neuromelanin-positive neurons from SNpc exhibited moderate Pan-DMT1 immunoreactivity (dark gray; *Upper*), whereas those from VTA (*Lower*) had scarce immunostaining. (*B*) DMT1 expression in SNpc neuromelanin-positive neurons in a PD subject (images representative of 7 patients studied). Pan-DMT1 immunostaining in neuromelanin-positive neurons (*Top*) was comparable to control. Pan-DMT1 was found in neuromelanin-positive neurons with and without Lewy bodies (arrows). PD patients also exhibited abundant labeling in small cells (<10 μm; arrowheads) in the ventral aspects of the SNpc. DMT1 +IRE immunolabeling (*Middle* and *Bottom Right*) localized like Pan-DMT1 immunoreactivity. The presence of iron accumulation in neuromelanin-positive neurons (arrows) and glial cells (arrowheads) in subjects studied was confirmed by Perls staining (blue; *Bottom*). (*C*) Colocalization of microglial marker CD68 (green) and Pan-DMT1 (magenta). (Scale bar and *Inset* width: *A* and *B*, 60 μm; *C*, 5 μm.) (*D*) DMT1 +IRE and −IRE immunoblots using extract of SNpc of controls and PD patients. Deglycosylation control using peptide *N*-glycosidase F (PNGase) (first lane of immunoblot). Bar charts quantify iron content and DMT1 blots normalized by actin in controls (black; $n = 7$) and PD patients (white; $n = 7$). **, $P < 0.01$.

postmortem tissue. When control subjects were examined (Fig. 1*A*), DMT1 antibodies directed against epitopes common to the 4 isoforms (hereinafter called Pan-DMT1) showed a moderate labeling in SNpc neuromelanin-containing DNs, with sparse staining in glial cells. Notably, DMT1 immunolabeling was consistently less intense in neuromelanin-containing DNs of the ventral tegmental area (VTA) than in those of the SNpc in the same tissue sections. In the mesencephalon of PD patients with iron accumulation confirmed by Perls staining (Fig. 1*B*), remaining neuromelanin-containing DNs exhibited DMT1 labeling that was comparable overall to that seen in controls. However, DNs localized in the ventral tier of the SNpc often exhibited strong labeling. Furthermore, light DMT1 staining was observed in the halo of Lewy bodies in the SNpc of PD patients (Fig. 1*B*). In addition to the DMT1 expression in DNs, small cells (diameter < 10 μm) showed strong labeling. When we used antibodies selective for DMT1 C-terminal isoforms, the pattern of immunolabeling for the +IRE isoform was comparable to that observed with Pan-DMT1 antibodies (Fig. 1*B*), whereas −IRE immunolabeling was consistently weaker and restricted to neuromelanin-positive DNs (data not shown). To identify nonmelanized cells with DMT1 labeling, double immunolabeling was performed for DMT1 and CD68 (a microglial marker) or glial fibrillary acidic protein (an astrocyte marker). Numerous $CD68^+/DMT1^+$ cells exhibiting amoeboid phagocytic morphology were observed in the ventral aspects of the SNpc in PD patients (Fig. 1*C*). In contrast, $CD68^+$ with scarce or no DMT1 labeling corresponded to the morphology of resting microglial cells, suggesting a link between DMT1 expression and microglial activation. No colocalization between DMT1 and glial fibrillary acidic protein was found in the samples analyzed (data not shown).

To quantify differences in DMT1 expression in the whole SNpc, Western blot analysis was performed on protein extracts prepared from the SNpc of control and PD patients (Fig. 1*D*). Western blot analysis for DMT1 revealed 2 bands, 65 and 90 kDa (Fig. 1*D*), matching the expected sizes for unmodified and glycosylated forms of this protein (20). We found that DMT1 +IRE was significantly increased in PD subjects compared with control subjects (Fig. 1*D*). On the other hand, DMT1 −IRE expression was significantly decreased (Fig. 1*D*), whereas no significant difference was observed for Pan-DMT1 expression (data not shown) when PD subjects were compared to control subjects. To corroborate the existence of iron accumulation in these PD patients, total iron content was tabulated (Fig. 1*D*) after atomic absorbance spectroscopy (AAS) analysis of whole-SNpc homogenates. Total iron content was significantly higher in PD patients than in age-matched controls (293.8 ± 13.9 ng/mg of protein and 203.8 ± 12.8 ng/mg of protein; $P < 0.01$).

DMT1 +IRE Is Up-Regulated in the Ventral Mesencephalon of MPTP-Intoxicated Mice. Given the advanced state of DN loss in symptomatic PD patients, we used acute MPTP intoxication to examine changes in DMT1 expression in earlier stages of degeneration. This animal model enables evaluation of the influences of mitochondrial complex I inhibition and inflammation on DMT1 expression. The effect of MPTP intoxication was confirmed by stereological counting of cells expressing tyrosine hydroxylase (TH), the rate-limiting enzyme in dopamine synthesis. MPTP-intoxicated mice showed a significant decrease in TH-positive cells 1 day after MPTP intoxication and a further decrease that stabilized 4 days after MPTP intoxication (Fig. 2*B*), in agreement with results published by other investigators (21). Quantitation of DMT1 bands in MPTP-intoxicated mice demonstrated an increase in DMT1 expression at days 1 and 2 after MPTP intoxication (Fig. 2 *A* and *B*), detected in the figure with antibodies recognizing the +IRE isoform, but not −IRE DMT1. The prevalent effect was an increase in DMT1 as also detected with antibodies recognizing the third or fourth extra-

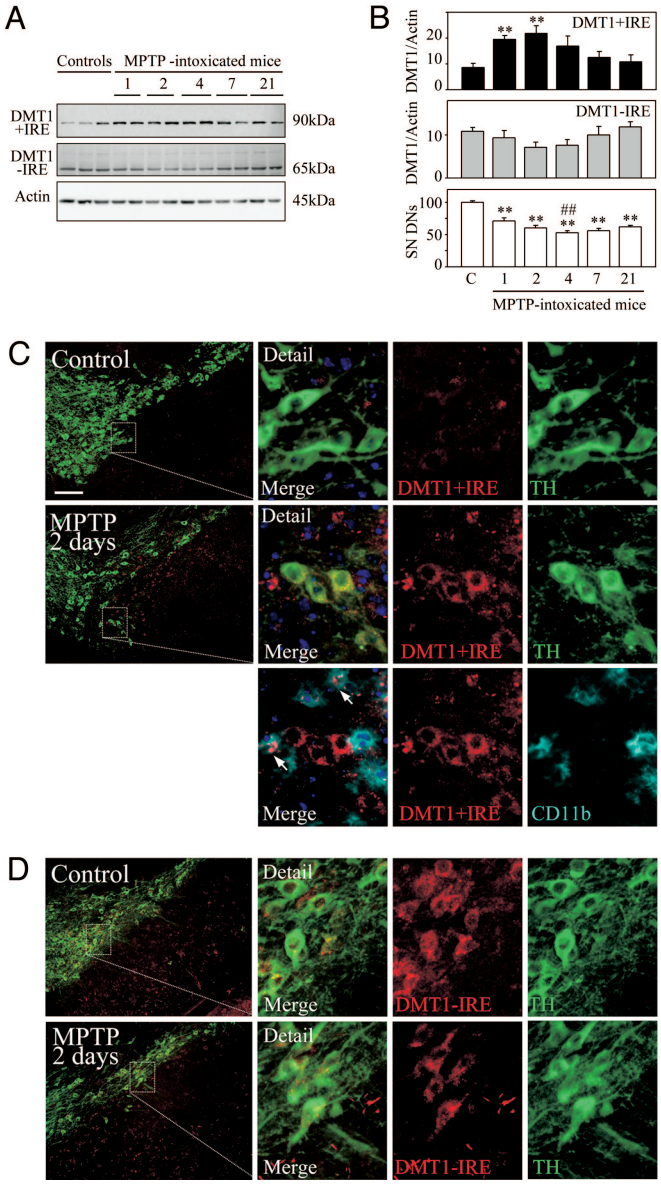

Fig. 2. DMT1 expression in the mesencephalon of MPTP-intoxicated mice. (*A*) Western blot analysis of DMT1 C-terminal isoforms and actin expression in ventral mesencephalon homogenates of control and MPTP-treated mice (n = 4 or 5 per day). (*B*) Time course of DMT1 +IRE and DMT1 −IRE expression changes (by immunoblot quantification; *Top* and *Middle*) and percentage of dopaminergic cell loss (by stereological cell counting of TH-positive DNs; *Bottom*) after acute MPTP intoxication. **, $P < 0.01$ compared with control; ##, $P < 0.05$ compared with day 1. (*C* and *D*) Localization of DMT1 isoforms and cell type-specific markers in the coronal mesencephalic sections of control and MPTP-treated mice. (*C*, *Top*) Modest DMT1 +IRE expression in the SNpc of control mice. (*C*, *Middle* and *Bottom*) DMT1 +IRE expression (red) in TH-positive dopaminergic neurons (green) and CD11b$^+$ activated microglia (cyan) 2 days after MPTP intoxication. (*D*, *Upper*) DMT1 −IRE expression (red) in TH-positive dopaminergic neurons (green) in the SNpc of control mice. (*D*, *Lower*) DMT1 −IRE expression (red) in TH-positive dopaminergic neurons (green) in SNpc 2 days after MPTP intoxication. (Scale bar and inset width: 100 μm.)

cellular domain (data not shown). The increase in DMT1 expression coincided with an increase in CD11b expression (data not shown), an index of microglial activation.

DMT1 +IRE Increases in DNs and Activated Microglia in the SNpc of MPTP-Intoxicated Mice. To identify cell types expressing DMT1 in control and MPTP-intoxicated mice, fluorescent double immunolabeling for DMT1 and selective cell type markers was performed in coronal brain sections. In agreement with Gunshin *et al.* (22), the cerebellum and the hippocampus were the structures with the strongest immunolabeling in normal mouse brain (data not shown). In the ventral mesencephalon from control mice, DMT1 +IRE immunolabeling was almost absent (Fig. 2*C Top*), whereas DMT1 −IRE presented a moderate labeling localized primarily in the DNs of the SNpc (Fig. 2*D Upper*) and in astrocytes in the SN pars reticulata (data not shown). One and 2 days after MPTP intoxication, DMT1 +IRE immunolabeling appeared in DNs and activated microglia in the SNpc (Fig. 2*C Middle* and *Bottom*). DMT1 −IRE immunoreactivity was observed in the remaining DNs (Fig. 2*D Right*) as well as in some reactive astrocytes (data not shown) in the SNpc at days 2 and 4 after MPTP intoxication.

Mesencephalic Iron Content Increases After Acute MPTP Intoxication. To examine whether DMT1 up-regulation correlates with changes in iron content, we assessed changes in total iron content and iron distribution in the ventral mesencephalon of MPTP-intoxicated mice. Reports of iron accumulation in the SNpc of MPTP-intoxicated monkeys (23) and of neuroprotection against MPTP achieved in mice by an iron-deficient diet (24) and iron chelators (5) support iron participation in MPTP-induced neurodegeneration. Total iron content of ventral mesencephalon analyzed by AAS was significantly increased 2 days after MPTP intoxication compared with control mice [77.4 ± 4.2 ng/mg of protein and 59.8 ± 4.0 ng/mg of protein, $P < 0.01$; supporting information (SI) Fig. S1*A*]. Using Perfusion–Perls with DAB enhancement, mild staining for iron developed on mesencephalic preparations from control mice (Fig. S1*B*), localized mainly in small cells (<10 μm) of the substantia nigra pars reticulata, whereas immunohistochemistry against TH revealed that TH-positive cells were consistently devoid of iron staining. However, in MPTP-intoxicated mice (Fig. S1*C*), cellular and extracellular iron staining was observed mainly localized in the anterior and ventral aspect of SNpc. Using confocal microscopy, we found: (*i*) DAB-positive cells with the size and topographic localization of DNs lacking TH immunolabeling; (*ii*) DAB-positive DNs with weak TH immunolabeling (detail in Fig. S1*C*); and (*iii*) small cells (diameter < 10 μm) with strong DAB staining and glial morphology. To evaluate the consequences of iron accumulation we performed immunohistochemistry against 4-hydroxynonenal and malondialdehyde (MDA) adducts in control and MPTP mice. At day 2 after MPTP intoxication, when iron accumulation was maximal, 4-hydroxynonenal (Fig. S1*D Right*) and MDA (data not shown) immunolabeling was found in the SNpc of MPTP mice. This staining was not observed in controls (Fig. S1*D Left*).

Mice Carrying a Mutation in DMT1 Are Partially Protected Against the Toxicity of MPTP. Even though DMT1 up-regulation in glial cells could have a protective effect by inducing iron sequestration, we hypothesize that its increase in DNs would probably contribute to the generation of oxidative stress and cell death. To test the hypothesis that DMT1 up-regulation contributes to iron-mediated MPTP toxicity, we assessed the susceptibility to MPTP of mycrocytic mice (*mk*/*mk*). The *mk*/*mk* mouse is a natural mutant that carries a mutation in the DMT1 gene (G185R) that results in a transporter with impaired iron transport. Homozygous *mk*/*mk* mice exhibited less susceptibility to MPTP compared with heterozygous (+/*mk*) and wild-type (+/+) littermates (25%, 58%, and 53% TH-positive cell loss compared with the respective saline-injected mice; Fig. 3 *A* and *B*). This difference in MPTP susceptibility was not explained by a difference in toxin bioavailability, because striatal concentrations of MPP$^+$ 90 min after MPTP administration were comparable in *mk*/*mk*, +/*mk*, and +/+ mice (6.8 ± 1.0 ng/mg of tissue, 7.2 ±

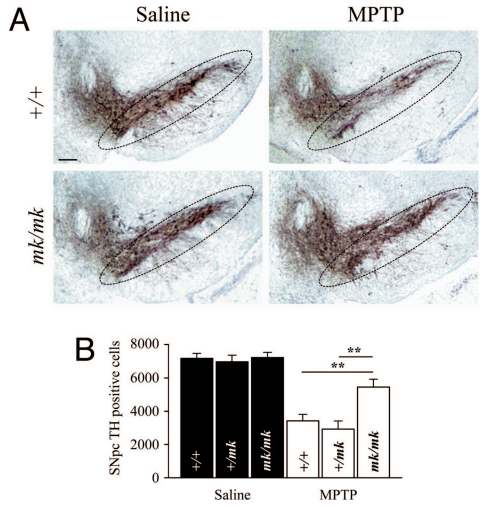

Fig. 3. MPTP-induced dopaminergic cell loss in +/+, +/*mk*, and *mk*/*mk* mice. (*A*) Peroxidase/DAB immunohistochemistry for TH on coronal mesencephalic sections from saline-injected and MPTP-intoxicated +/+ (WT) and *mk*/*mk* mice. The SNpc is delineated. (Scale bar: 100 μm.) (*B*) Bar graph of stereological counts of TH-positive cells in the SNpc of saline- and MPTP-injected mice (7 days after MPTP intoxication). **, $P < 0.01$.

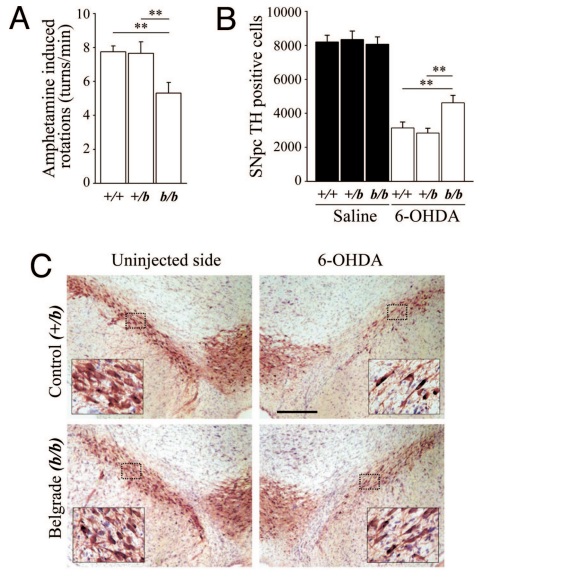

Fig. 4. Amphetamine-induced rotational behavior and dopaminergic cell loss in +/+, +/*b*, and *b*/*b* rats after 6-OHDA intrastriatal injection. (*A*) Bar graph of amphetamine-induced rotational behavior 7 days after 6-OHDA injection in wild-type Fischer 344 (+/+), heterozygous (+/*b*), and Belgrade (*b*/*b*) rats. (*B*) Bar graph of stereological nigral TH-positive DN counts in sham-injected and 6-OHDA-injected rats 14 days after injection. **, $P < 0.01$. (*C*) Representative peroxidase/DAB immunohistochemistry for TH on coronal mesencephalic sections +/*b* (control) and *b*/*b* (Belgrade) rats 14 days after 6-OHDA injection. (Scale bar: 300 μm.) (*Insets*) Enlargements of the outlined areas.

1.1 ng/mg of tissue, and 5.9 ± 0.9 ng/mg of tissue, respectively). Nevertheless, the difference in the loss of striatal dopamine content induced by MPTP between *mk*/*mk*, +/*mk*, and +/+ mice did not reach significance (61.0%, 76.6%, and 73.8% decrease in dopamine content compared with the respective saline-injected mice). Thus, these data rule out the possibility that the increase in functional DMT1 in +/+ and +/*mk* mice protects against DN damage and support the hypothesis that the increase actually leads to a toxicity that would not otherwise occur.

Belgrade Rats Carrying a Mutation in DMT1 Are Partially Protected Against the Toxicity of 6-OHDA. We previously described an increase in the expression of DMT1 in the ventral mesencephalon of rats after striatal 6-OHDA injections (25). To test whether DMT1 up-regulation increases iron-mediated toxicity in another PD animal model and to evaluate the behavioral impact of neuroprotection, we tested the susceptibility of Belgrade rats (*b*/*b*) to 6-OHDA neurotoxicity. Belgrade rats carry the same mutation in the DMT1 gene as that found in *mk*/*mk* mice. One week after unilateral intrastriatal stereotactic injection of 6-OHDA, amphetamine-induced rotation was measured in Belgrade rats, heterozygous littermates, and wild-type rats. Belgrade rats exhibited significantly less amphetamine-induced turning behavior than heterozygous and wild-type rats (5.3 ± 0.6 turns per min, 7.7 ± 0.6 turns per min, and 7.5 ± 0.3 turns per min, respectively; $P < 0.01$; Fig. 4*A*), consistent with less DA depletion. SN dopaminergic cell loss was assessed when the lesion had stabilized 2 weeks after 6-OHDA administration. Belgrade rats showed a significantly smaller degree of lesion compared with those of heterozygous and wild-type rats (42.6%, 65.9%, and 61.6% of SNpc DNs, respectively, compared with sham-operated animals; Fig. 4 *B* and *C*). Sham-operated rats did not exhibit rotational behavior or a significant loss of TH-positive cells compared with the noninjected side (data not shown).

Discussion

DMT1 Expression Is Increased During DN Degeneration. In this study we describe the expression of DMT1 isoforms in the SNpc of control and PD patients. In control subjects, moderate DMT1 immunolabeling was found in the SNpc and associated predominantly with neuromelanin-containing DNs, in agreement with the distribution reported in a previous study in nonhuman primates (26). Yet, only a light DMT1 staining was reported in that study (26). The slight discrepancy in DMT1 expression level in DNs is likely explained by differences in the relative ages of the groups studied. DMT1 expression has been reported to increase with age (11); our patients were older than 60 years, whereas the monkeys corresponded to young human adults. Notably, DNs from the VTA consistently displayed less intense DMT1 immunolabeling than DNs from the SNpc. This finding is relevant in view of the known preferential vulnerability of SNpc DNs in PD compared with VTA neurons (27). Higher DMT1 expression in nigral DNs and consequently higher iron levels in these neurons may thus constitute a factor that increases the vulnerability of nigral neurons to PD-related insults.

In the SNpc of PD patients, DMT1 +IRE expression was found to be increased when compared with that of age-matched controls, as assessed by Western blot analysis. Immunohistochemical analysis showed DMT1 labeling in remaining DNs that was particularly strong in some neurons from the ventral part of the SNpc, whereas additional DMT1 labeling appeared in activated microglia, as shown by colocalization with CD68. Moreover, in matched samples, iron content paralleled DMT1 +IRE expression. Thus, our results suggest that nigral DMT1 expression was increased in PD patients, most likely because of DMT1 up-regulation in reactive glia and surviving DNs of the ventral SNpc. To explore the role of this increase in DMT1 expression, we used the MPTP mouse model of PD that recapitulates several features of the disease. In acutely MPTP-intoxicated mice, we observed that: (*i*) DMT1 up-regulation was an early but continuing occurrence during neuronal death; (*ii*) DMT1 +IRE but not −IRE was up-regulated in SNpc DNs; and (*iii*) +IRE and −IRE isoforms were expressed, respectively, by activated microglia and hypertrophic astrocytes during the same time period. Taken together with the reported DMT1 up-regulation in the mesencephalon of 6-OHDA-lesioned rats (25), our results sug-

gest that DMT1 increase is associated with DN degeneration and is a common phenomenon in animal models of PD.

To examine whether DMT1 is instrumental in the neuronal death in rodent models of PD, we made use of rodent mutants carrying a mutation that impairs DMT1 iron transport. These rodents exhibit a significant alteration in the kinetics of brain iron incorporation (28). Nevertheless, although a decrease in Perls iron histochemistry has been reported in the brain of Belgrade rats (29), quantitative techniques detect only mild or nonsignificant decreases in brain iron content in Belgrade rats and *mk*/*mk* mice, respectively (ref. 28; data not shown). Consequently, brain development and iron-dependent processes, such as myelin and dopamine synthesis, appear normal in DMT1 G185R mutant rodents (data not shown). We found that *mk*/*mk* mice were partially protected against MPTP toxicity. These results are consistent with resistance to MPTP reported in mice on an iron-deficient diet (24). However, dietary iron deficiency has been independently associated with a significant decrease in mesencephalic iron and striatal dopamine content, the latter deficit being explained by the fact that iron is a required cofactor of TH (24, 30). In contrast, mesencephalic iron content and striatal dopamine content in *mk*/*mk* mice were not significantly different from those of +/*mk* and +/+ mice (data not shown), likely because of the existence of compensatory mechanisms. Finally, using the 6-OHDA model of PD, we found that DMT1 deficiency in *b*/*b* rats conferred a partial protection against intrastriatal 6-OHDA toxicity. Moreover, neuroprotection in *b*/*b* rats may have a functional impact, because lesioned mutant rats exhibited less amphetamine-induced rotational behavior than lesioned control rats. Belgrade rats received an iron-supplemented diet to palliate systemic iron deficiency; nonetheless, we cannot fully rule out the possibility that anemia may have contributed to some extent to the behavioral difference observed. Collectively, these data indicate that DMT1-mediated iron transport is involved in neuronal degeneration in parkinsonian syndromes and that DMT1 deficiency mitigates cell death and may have functional consequences.

Possible Mechanisms Involved in the Death of DNs Mediated by DMT1 Iron Transport. The increase of DMT1 in the mesencephalon preceded and coincided with the increase in iron content in MPTP-intoxicated mice, suggesting that DMT1 contributes to iron accumulation. Moreover, the distribution of DMT1 +IRE expression coincided with that of iron accumulation observed by iron histochemistry in the ventral SNpc of MPTP mice. Local iron toxicity is due primarily to the production (through the Fenton reaction) of hydroxyl radicals, responsible for oxidation of lipids, proteins, and DNA (31). Such a hypothesis is in agreement with our results, where DMT1 up-regulation and iron accumulation in SNpc DNs of MPTP-treated mice were associated with lipoperoxidation, as evidenced by the presence of 4-hydroxynonenal and MDA adducts. Our data are consistent with postmortem studies showing increased lipoperoxidation, protein carbonylation, and DNA oxidation in the SNpc of PD patients (31). DMT1 participation in DN death is thus likely to involve iron-mediated induction of oxidative stress.

What Are the Mechanisms Underlying DMT1 Up-Regulation in PD? Several mechanisms may account for the increase in DMT1 expression in DNs and glial cells in PD. First, inhibition of mitochondrial complex I, a phenomenon reported in PD and the primary event in MPTP neurotoxicity, can directly modulate neuronal DMT1 expression. MPTP-associated inhibition of mitochondrial complex I can cause both a rise in reactive oxygen and nitrogen species and ATP depletion (17). These 2 events can augment the binding activity (32, 33) of iron regulatory proteins (IRPs) that control the expression of DMT1 +IRE and the subsequent increase in iron content (34). Although a genomic study failed to show DMT1 up-regulation in an M9D dopaminergic cell line treated with MPP^+ (35), a more recent study using MES23.5 dopaminergic cells indicated that MPP^+ was sufficient to increase DMT1 expression and iron uptake (36). Second, DMT1 expression may be influenced by neuroinflammatory processes that are reported to occur in PD and to contribute to MPTP-induced neurodegeneration (16). Indeed, proinflammatory stimuli, such as exposure to lipopolysaccharide or cytokines such as TNF-α or IFN-γ, are effective at up-regulating DMT1 in multiple cell types (12–15), including phagocytic cells. Such a modulation of DMT1 expression is compatible with our results, particularly where DMT1 up-regulation coincided with microglial activation at days 1 and 2 after MPTP intoxication. Even if modulation of proinflammatory stimuli is more likely to affect glial DMT1 expression, we cannot exclude a direct effect of proinflammatory cytokines on neuronal DMT1 expression. Indeed, TNF-α receptor expression has been reported in human SNpc DNs (37).

What Is the Mechanism of DMT1-Mediated Iron Transport in PD? A model has been proposed for iron incorporation in which DMT1 +IRE might participate preferentially in NTBI uptake and DMT1 −IRE in TBI uptake (38). In the SN, the expression of TfR and the density of Tf-binding sites are relatively low in normal SN and further decrease in the brain of PD patients (8). On the other hand, we here report the existence of DMT1 +IRE in the SN and its increase in PD and animal models of the disease. Furthermore, the existence of ferrous NTBI has been well documented in normal brain. Thus, we hypothesize that DMT1 +IRE-mediated iron toxicity might implicate NTBI transport in the SN.

Several mechanisms may contribute to increase iron transport mediated by DMT1 in PD. DMT1 is a ferrous-iron transporter with conductance described as temperature-, H^+-, and voltage-dependent. (*i*) DMT1 transport capacity is optimal at pH 5.5. Yet, it is also capable of transporting iron at neutral pH (39, 40), the situation observed in PD brain. (*ii*) DMT1 iron transport depends on the membrane potential, increasing with hyperpolarization (22, 40). Because MPTP and 6-OHDA treatments induce hyperpolarization of dopaminergic neurons by means of the activation of ATP-sensitive potassium channels (41, 42), we hypothesize that this hyperpolarization can participate as a driving force of DMT1 iron transport. (*iii*) In addition, NMDA and neuronal nitric oxide synthase (nNOS) activation has recently been invoked in a DMT1-dependent stimulation of iron uptake in neurons (43). Because NMDA agonism and nNOS activation are likely involved in the death of DNs in PD (44), this modulation could also contribute to increase DMT1 iron transport in parkinsonian syndromes. As a consequence, it might be hypothesized that neuroprotection associated with DMT1 deficiency might result, at least in part, from a lesser response to hyperpolarization and excitotoxic stimuli.

In summary, our results support a general role for DMT1 in neurodegeneration associated with PD and confirm the role of iron in the progression of neuronal death in parkinsonian syndromes. Increased DMT1 expression during aging may also explain in part why aging is the major risk factor for developing PD (11). Consequently, DMT1 represents a promising molecular target for the design of therapeutic interventions that would slow PD progression.

Materials and Methods

Chemicals and Antibodies. See *SI Materials and Methods*.

Human Postmortem Tissue. Brains were obtained postmortem from control individuals with no known history of neurological or psychiatric disorders and from patients with clinically defined PD [stages II to IV on the rating scale of Hoehn and Yahr (45) responding to levodopa therapy] that was histologically confirmed (nigral neuronal loss; presence of Lewy bodies in the SN and locus ceruleus). For immunohistochemistry, we studied 7 PD patients and 6 controls

matched for age (80.7 ± 2.5 years and 78.3 ± 3.2 years, respectively) and postmortem delay (36.0 ± 5.3 h and 35.7 ± 4.7 h, respectively). For Western blot analysis and AAS iron measurements, we analyzed the specimens from 7 parkinsonian patients and 7 controls with comparable ages at death (81.2 ± 4.7 years and 70.5 ± 3.9 years, respectively) and postmortem delay (16.4 ± 3.2 h and 16.5 ± 3.8 h, respectively).

Tissue Preparation for AAS Iron Measurement and Western Blotting. See *SI Materials and Methods*.

Tissue Preparation for Immunohistochemistry and Perls Staining. See *SI Materials and Methods*.

Immunohistochemistry. See *SI Materials and Methods*.

Animals. See *SI Materials and Methods*.

MPTP Intoxication. Mice were injected i.p. 4 times (at 2-h intervals over 1 day) with 20 mg/kg MPTP free base in saline or a corresponding volume of saline alone. At selected time points, animals were killed and the ventral mesencephali of control and MPTP-intoxicated mice were dissected out: one hemisphere was used for biochemical analysis and the other was used for stereological quantification of SNpc DNs.

6-OHDA Lesions. The lesions were generated by unilateral striatal injection of 20 μg of 6-OHDA (4 μg/μL calculated as free base, in 0.2 mg/mL ascorbic acid/saline) or a corresponding volume of vehicle. The coordinates for the injection site, calculated from the bregma by using the rat brain atlas of Paxinos and Watson (46), for the anteroposterior, mediolateral, and dorsoventral positions were as follows: +1.0, −3.0, and 5.0, respectively.

HPLC Measurement of Dopamine and MPP^+. See *SI Materials and Methods*.

Amphetamine-Induced Rotation. See *SI Materials and Methods*.

Image Analysis and Stereological Cell Counting. See *SI Materials and Methods*.

Protein Deglycosylation, Western Blots, and Quantification. See *SI Materials and Methods*.

AAS and Perfusion–Perls. See *SI Materials and Methods*.

Statistics. Data are shown as mean ± SEM. Normal parametric data were compared with the 2-sided, unpaired *t* test or ANOVA followed by post-hoc Holm–Sidak test. $P < 0.05$ was considered significant.

ACKNOWLEDGMENTS. We thank Funmei Yang and Mark Fleming for breeding stock of microcytic mice. This work was supported by the Institut National de la Santé et de la Recherche Médicale, the Laura and Michael Garrick Fund, the Program Alban, the European Union Program of High-Level Scholarships for Latin America, scholarship E04D044044CL, and l'Association France Parkinson.

1. Forno LS (1996) Neuropathology of Parkinson's disease. *Neuropathol Exp Neurol* 55:259–272.
2. Sofic E, *et al.* (1988) Increased iron (III) and total iron content in post mortem substantia nigra of parkinsonian brain. *J Neural Transm* 74:199–205.
3. Hirsch EC, Brandel JP, Galle P, Javoy-Agid F, Agid Y (1991) Iron and aluminum increase in the substantia nigra of patients with Parkinson's disease: An X-ray microanalysis. *J Neurochem* 56:446–451.
4. Uversky VN, Li J, Fink AL (2001) Metal-triggered structural transformations, aggregation, and fibrillation of human alpha-synuclein. A possible molecular link between Parkinson's disease and heavy metal exposure. *J Biol Chem* 276:44284–44296.
5. Kaur D, *et al.* (2003) Genetic or pharmacological iron chelation prevents MPTP-induced neurotoxicity in vivo: A novel therapy for Parkinson's disease. *Neuron* 37:899–909.
6. Taylor EM, Crowe A, Morgan EH (1991) Transferrin and iron uptake by the brain: Effects of altered iron status. *J Neurochem* 57:1584–1592.
7. Hill JM, Ruff MR, Weber RJ, Pert CB (1985) Transferrin receptors in rat brain: Neuropeptide-like pattern and relationship to iron distribution. *Proc Natl Acad Sci USA* 82:4553–4557.
8. Faucheux BA, Hauw JJ, Agid Y, Hirsch EC (1997) The density of [^{125}I]-transferrin binding sites on perikarya of melanized neurons of the substantia nigra is decreased in Parkinson's disease. *Brain Res* 749:170–174.
9. Garrick LM, Dolan KG, Romano MA, Garrick MD (1999) Non-transferrin-bound iron uptake in Belgrade and normal rat erythroid cells. *J Cell Physiol* 178:349–358.
10. Hubert N, Hentze MW (2002) Previously uncharacterized isoforms of divalent metal transporter (DMT)-1: Implications for regulation and cellular function. *Proc Natl Acad Sci USA* 99:12345–12350.
11. Ke Y, *et al.* (2005) Age-dependent and iron-independent expression of two mRNA isoforms of divalent metal transporter 1 in rat brain. *Neurobiol Aging* 26:739–748.
12. Ludwiczek S, Aigner E, Theurl I, Weiss G (2003) Cytokine-mediated regulation of iron transport in human monocytic cells. *Blood* 101:4148–4154.
13. Wardrop SL, Richardson DR (2000) Interferon-gamma and lipopolysaccharide regulate the expression of Nramp2 and increase the uptake of iron from low relative molecular mass complexes by macrophages. *Eur J Biochem* 267:6586–6593.
14. Wang X, *et al.* (2005) TNF, IFN-gamma, and endotoxin increase expression of DMT1 in bronchial epithelial cells. *Am J Physiol* 289:L24–L33.
15. Nanami M, *et al.* (2005) Tumor necrosis factor-alpha-induced iron sequestration and oxidative stress in human endothelial cells. *Arterioscler Thromb Vasc Biol* 25:2495–2501.
16. Hunot S, Hirsch EC (2003) The role of glial reaction and inflammation in Parkinson's disease. *Ann Neurol* 53(suppl 3):S49–S58.
17. Przedborski S, Tieu K, Perier C, Vila M (2004) MPTP as a mitochondrial neurotoxic model of Parkinson's disease. *J Bioenerg Biomembr* 36:375–379.
18. Fleming MD, *et al.* (1997) Microcytic anaemia mice have a mutation in Nramp2, a candidate iron transporter gene. *Nat Genet* 16:383–386.
19. Fleming MD, *et al.* (1998) Nramp2 is mutated in the anemic Belgrade (b) rat: Evidence of a role for Nramp2 in endosomal iron transport. *Proc Natl Acad Sci USA* 95:1148–1153.
20. Tabuchi M, Tanaka N, Nishida-Kitayama J, Kishi F (2002) Alternative splicing regulates the subcellular localization of divalent metal transporter 1 isoforms. *Mol Biol Cell* 13:4371–4387.
21. Jackson-Lewis V, Jakowec M, Burke RE, Przedborski S (1995) Time course and morphology of dopaminergic neuronal death caused by the neurotoxin 1-methyl-4-phenyl-1,2,3,6-tetrahydropyridine. *Neurodegeneration* 4:257–269.
22. Gunshin H, *et al.* (1997) Cloning and characterization of a mammalian proton-coupled metal-ion transporter. *Nature* 388:482–488.
23. He Y, *et al.* (2003) Dopaminergic cell death precedes iron elevation in MPTP-injected monkeys. *Free Radic Biol Med* 35:540–547.
24. Levenson CW, *et al.* (2004) Role of dietary iron restriction in a mouse model of Parkinson's disease. *Exp Neurol* 190:506–514.
25. Salazar J, Mena N, Nuñez MT (2006) Iron dyshomeostasis in Parkinson's disease. *J Neural Transm Suppl* 71:205–213.
26. Huang E, Ong WY, Connor JR (2004) Distribution of divalent metal transporter-1 in the monkey basal ganglia. *Neuroscience* 128:487–496.
27. Hirsch E, Graybiel AM, Agid YA (1988) Melanized dopaminergic neurons are differentially susceptible to degeneration in Parkinson's disease. *Nature* 334:345–348.
28. Moos T, Morgan EH (2004) The significance of the mutated divalent metal transporter (DMT1) on iron transport into the Belgrade rat brain. *J Neurochem* 88:233–245.
29. Burdo JR, *et al.* (1999) Cellular distribution of iron in the brain of the Belgrade rat. *Neuroscience* 93:1189–1196.
30. Unger EL, *et al.* (2007) Early iron deficiency alters sensorimotor development and brain monoamines in rats. *J Nutr* 137:118–124.
31. Jenner P (2003) Oxidative stress in Parkinson's disease. *Ann Neurol* 53(suppl 3):S26–S36.
32. Hentze MW, Kühn LC (1996) Molecular control of vertebrate iron metabolism: mRNA-based regulatory circuits operated by iron, nitric oxide, and oxidative stress. *Proc Natl Acad Sci USA* 93:8175–8182.
33. Bouton C, Chauveau MJ, Lazereg S, Drapier JC (2002) Recycling of RNA binding iron regulatory protein 1 into an aconitase after nitric oxide removal depends on mitochondrial ATP. *J Biol Chem* 277:31220–31227.
34. Galy B, Ferring-Appel D, Kaden S, Grone HJ, Hentze MW (2008) Iron regulatory proteins are essential for intestinal function and control key iron absorption molecules in the duodenum. *Cell Metab* 7:79–85.
35. Wang J, *et al.* (2007) Gene expression profiling of MPP^+-treated MN9D cells: A mechanism of toxicity study. *Neurotoxicology* 28:979–987.
36. Zhang S, Wang J, Song N, Xie J, Jiang H (2008) Up-regulation of divalent metal transporter 1 is involved in 1-methyl-4-phenylpyridinium (MPP^+)-induced apoptosis in MES23.5 cells. *Neurobiol Aging*, in press.
37. Boka G, *et al.* (1994) Immunocytochemical analysis of tumor necrosis factor and its receptors in Parkinson's disease. *Neurosci Lett* 172:151–154.
38. Lam-Yuk-Tseung S, Gros P (2006) Distinct targeting and recycling properties of two isoforms of the iron transporter DMT1 (NRAMP2, Slc11A2). *Biochemistry* 45:2294–2301.
39. Garrick MD, *et al.* (2006) Comparison of mammalian cell lines expressing distinct isoforms of divalent metal transporter 1 in a tetracycline-regulated fashion. *Biochem J* 398:539–546.
40. Mackenzie B, Ujwal ML, Chang MH, Romero MF, Hediger MA (2006) Divalent metal-ion transporter DMT1 mediates both H^+-coupled Fe^{2+} transport and uncoupled fluxes. *Pflügers Arch* 451:544–558.
41. Liss B, *et al.* (2005) K-ATP channels promote the differential degeneration of dopaminergic midbrain neurons. *Nat Neurosci* 8:1742–1751.
42. Berretta N, *et al.* (2005) Acute effects of 6-hydroxydopamine on dopaminergic neurons of the rat substantia nigra pars compacta in vitro. *Neurotoxicology* 26:869–881.
43. Cheah JH, *et al.* (2006) NMDA receptor-nitric oxide transmission mediates neuronal iron homeostasis via the GTPase Dexras1. *Neuron* 51:431–440.
44. Beal MF (1998) Excitotoxicity and nitric oxide in Parkinson's disease pathogenesis. *Ann Neurol* 44:S110–S114.
45. Hoehn MM, Yahr MD (1967) Parkinsonism: Onset, progression and mortality. *Neurology* 17:427–442.
46. Paxinos G, Watson C (1986) *The Rat Brain in Stereotaxic Coordinates* (Academic, San Diego, 2nd Ed).